How to Use Trim Quads to Modify Dispersion

D. Douglas

Abstract

Remnant dispersion errors have been observed in the FEL driver recirculator [1]. These errors will affect M_{56} control and may lead to spot size growth during energy recovery. We describe how compensatory dispersion trims can be generated using end-loop trim quadrupoles.

Overview

The FEL driver transport system has eight QH trim quadrupoles. These are installed in the end loops (3F and 5F regions) and nominally are to be operated in two families (3F01/3F04/5F01/5F04 and 3F02/3F03/5F02/5F03) to allow control of recirculator dispersion and momentum compaction. In the event that inadvertent dispersion errors arise, they can be individually set to provide an intentional dispersion wave that offsets the observed dispersion error. In the following, we describe how such dispersion trims can be implemented.

Nominal Optics

Beam envelopes for the nominal machine optics are shown in Figure 1. The initial beam envelopes are obtained by back-propagation of wiggler matched values through 1F03 – 2F03 quad excitations used during the summer 1998 running period. The envelopes are then forward propagated through a quasi-isochronous tuning of the recirculator (M_{56} = 0 from wiggler to re-injection point; trim quads are off), using the 2F04 – 2F09 telescope to match into the machine backleg. The 5F05 – 5F08 telescope is used to control the envelopes during energy recovery. Quadrupole excitations for this solution are given in Table 1 of the Appendix.

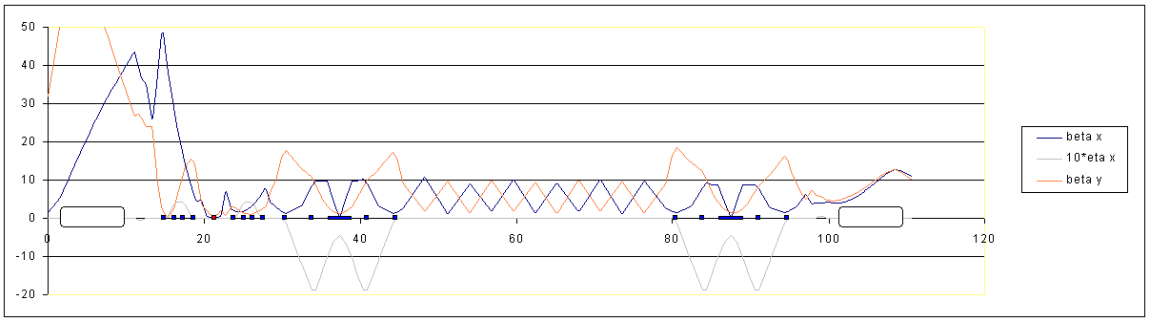

Figure 1: Beam envelopes and dispersions for nominal machine optics.

This solution is dispersion suppressed in the backleg and at re-injection. As described elsewhere [2], this quasi-isochronous tuning will not lead to acceptable performance after energy recovery. Energy compression must be implemented through proper choice of linear and quadratic momentum compaction to avoid beam loss at the 1G dump. The implementation of this energy compression (in particular, the required M_{56} value) depends on details (such as the sign of beam matrix Σ_{56} after the injector and the side of cryomodule crest phase on which acceleration occurs) which are at the time of this note, not yet clear. However, certain characteristics of the compaction management system should be present in all cases and can be used to debug and certify transport system performance.

As discussed in Reference [2], the quad pairs in the second trim family (QH3F02/3 and QH5F02/3) lie across 180^o bends from one another. Thus, systematic excitation of these magnets will dramatically change machine momentum compaction without significantly affecting dispersion. Figure 2 illustrates a rudimentary energy recovery mode, with M_{56} = 0.2 m from wiggler to re-injection point set by use of a single trim quad family. This solution is obtained from that in Figure 1 by simply exciting QH(3/5)F0(2/3) to $k_1 = -0.17/m^2$. There is some induced beam envelope mismatch; this can be compensated using the 2F04/9 and 5F05/8 telescopes, as shown in Figure 3 (new quad values are given in Table 2 of the Appendix).

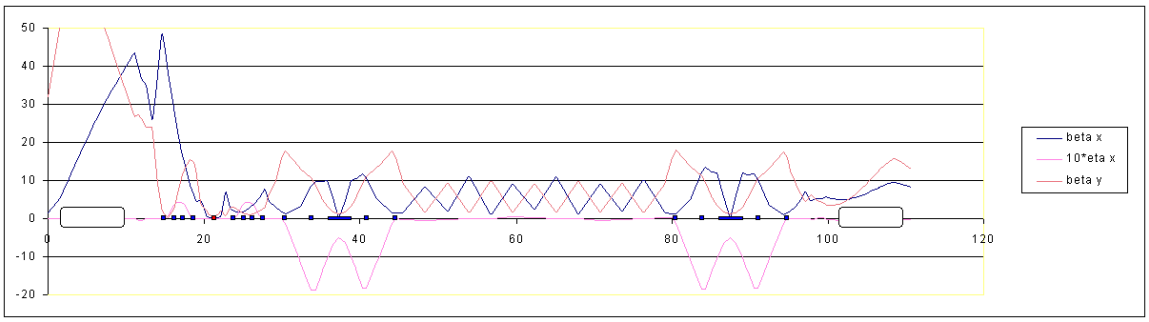

Figure 2: Rudimentary energy recovery mode - uses one trim quad family.

Failure of the transport system to conform to this behavior indicates the presence of an error. A simple blunder leading to violation of the expected dispersion suppression is a polarity error in the downstream trim quad. If we excite QH3F03 to +0.17/ m^2, the downstream transport exhibits a significant dispersion wave. This is shown in Figure 4. Similarly, misalignments (such as significant longitudinal misplacement [3] and mispowering of the 180^o dipoles) can lead to dispersion errors and lack of proper response to trim quad excitations.

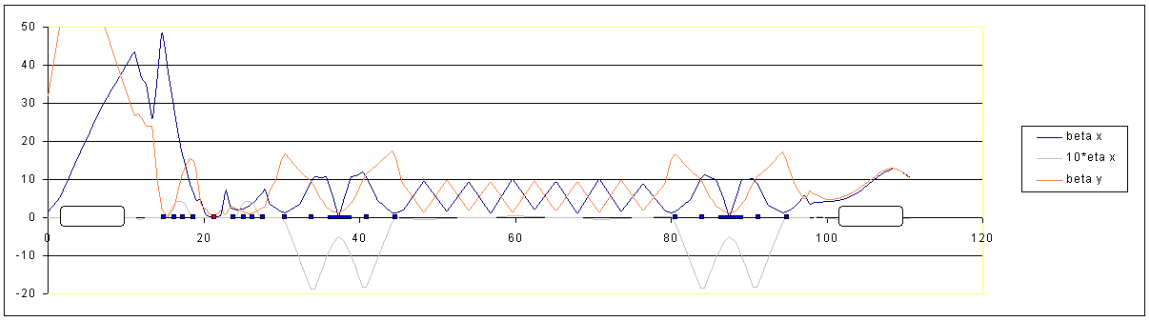

Figure 3: Rudimentary energy recovery mode with re-matching.

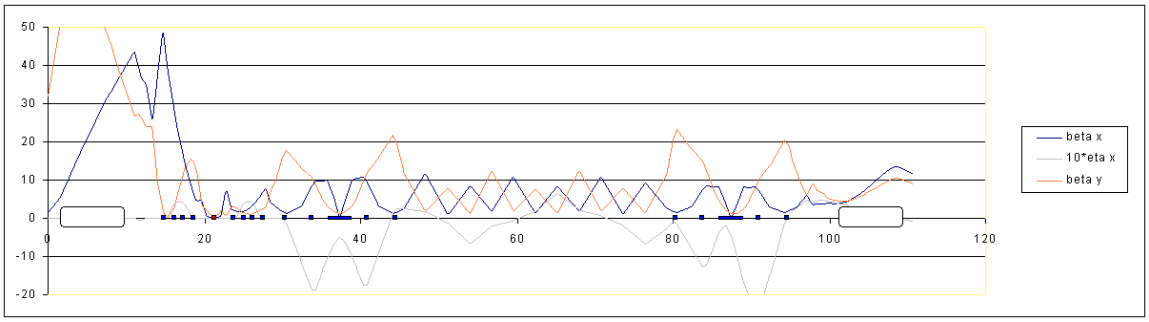

Figure 4: Effect of polarity error in QH3F03.

Dispersion Trims

Individual trim quads can be excited to generate dispersion in the backleg and at the re-injection point. Use of two trim quads can lead to "sine-like" and "cosine-like" dispersive orbits in each of these regions. Using the Excel-based machine model [4], one can quickly evaluate various schemes for generating dispersion compensations. Furthermore, re-matching of beam envelopes in the backleg and at re-injection can be rapidly performed using the same model. We now give examples.

Sine-like dispersion wave in backleg (h' at 4F01) – A dispersive slope at 4F01 is readily generated using QH3F01 and QH3F04. Figure 5 illustrates the result of setting QH3F01 to $k_1 = 0.5/m^2$ and QH3F04 to $k_1 = 0.1/m^2$. The resulting dispersion wave has a node at 4F01 and is nonzero ¾ betatron wavelength away at 4F07. Starting with nominal (Table 1) values, beam envelopes are readily controlled by adjusting QB2F06 to $-8.3/m^2$ and QG2F07 to $+4.2/m^2$ in order to restore the backleg match. The result is shown in Figure 6.

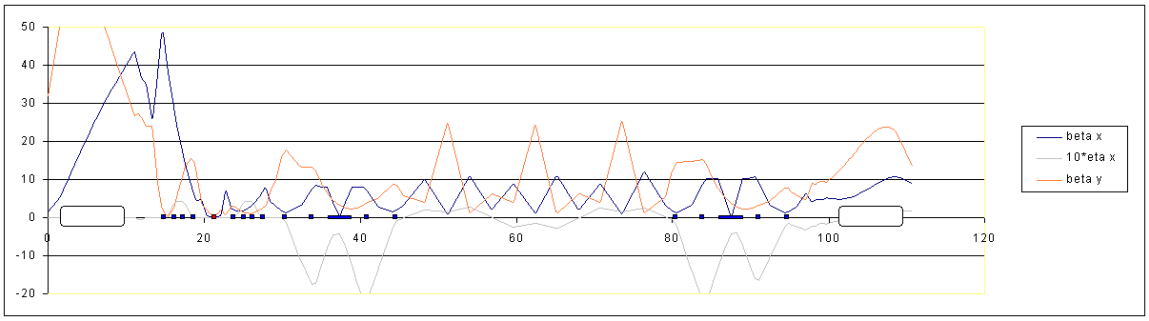

Figure 5: η' at 4F01, sine-like dispersion through backleg

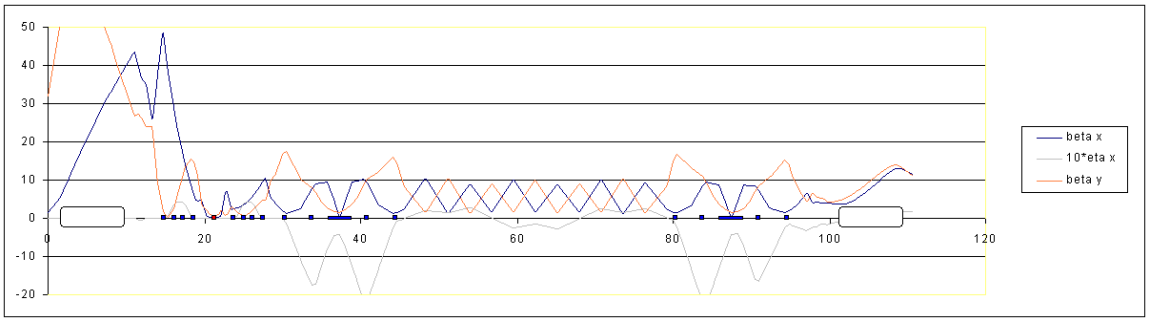

Figure 6: Solution of Figure 5 with envelopes re-matched using QB2F06 and QB2F07.

Cosine-like dispersion wave in backleg (h at 4F01) – Dispersion at 4F01 is readily generated using QH3F01 and QH3F02. Figure 7 illustrates the result of setting QH3F01 to $k_1 = 0.8/m^2$ and QH3F02 to $k_1 = -0.6/m^2$. The resulting dispersion wave is nonzero at 4F01 and is has a node ¾ betatron wavelength away at 4F07. Beam envelopes are, as in the previous example, readily controlled by changing upstream matching quads. In this case, QB2F06 and QG2F09 are adjusted to restore the periodic match in the backleg. The result is presented in Figure 8.

Conclusions

In a properly executed driver lattice, use of rudimentary momentum compaction trims will not significantly alter dispersion. The presence of error dispersions through the machine indicates the existence of some lattice error, such as a trim quad polarity error or construction/installation error in dipoles. Error dispersions can be readily corrected; the betatron mismatch induced during such correction can be simply compensated.

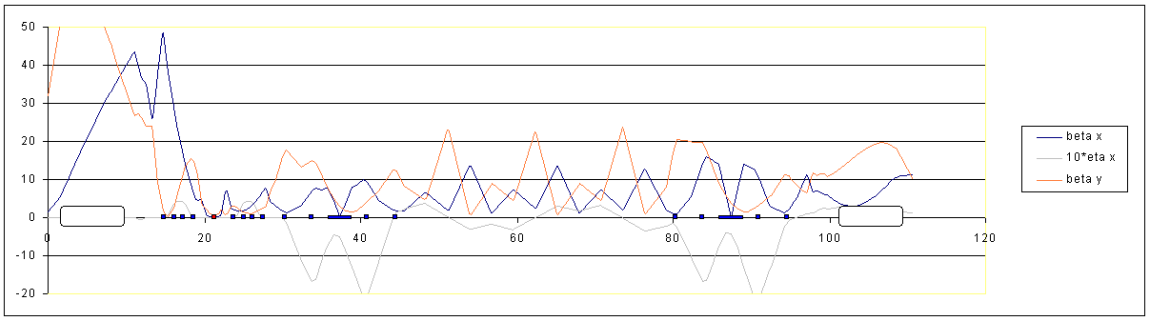

Figure 7: η at 4F01, cosine-like dispersion through backleg.

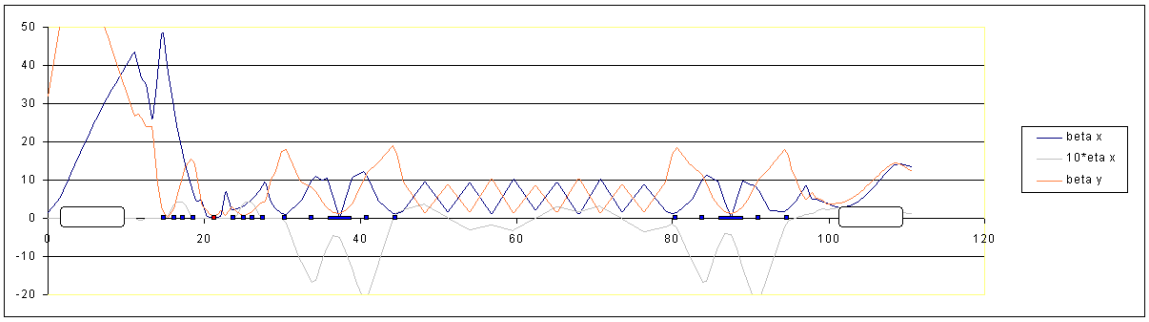

Figure 8: Solution of Figure 7 with envelopes re-matched using QB2F06 and QG2F09.

We note that as such schemes create η-waves through the end loops, they significantly modify the dispersion at nearly all trim quads. The results are therefore inherently nonlinear in the trim quad strength. For example, if one develops a “sine-like” dispersion wave in the backleg, simply reversing the polarity of the trim quad excitations does not produce a “sine-like” wave with opposite sign. Typically the magnitude of the second trim quad must be modified as well because of the change in the local dispersion and resulting change in response to variations in quad excitation.

References

[1] P. Piot, private communication and various FLOG entries in early August 1998.

[2] D. Douglas, “Lattice Issues Affecting Longitudinal Phase Space Management During Energy Recovery, Or, ‘Why the FEL Needs Sextupoles’”, JLAB-TN-98-025, 9 July 1998.

[3] We note that there is some evidence of a significant path length error in the end loops, possibly due to misplacement of the large DY dipoles. The

DG3F02H path length trim system has, in July/August 1998, persistently been excited to ~1400 g-cm, corresponding to 10 mrad steering through the DY magnets. This corresponds to a +4 cm correction to the path length, implying the machine is 4 cm short. A possible candidate source for this error is a misplacement of the DY magnets, in which the end of the iron does not precisely correspond to the end of the field. Such a misalignment would in turn lead to a dispersion error, due to path length errors between adjacent DQ magnets (which focus the dispersion significantly).

[4] D. Douglas, “An Alternate Paradigm for High-Level Application Development”, JLAB-TN-97-047, 12 December 1997.

Appendix

Table 1: “Nominal” Optics Magnet Settings

magnet or string	description	bl (g-cm) or b'l (g)
dipoles		
MDU1F02	extraction string	11018.49869
MDW2F01	optical cavity string	47952.11301
MDX3F01	first reverse bend	65148.80351
MDX2G01	trim on first reverse bend	set to 0 current
MDY3F03	C-bend	403563.4618
quadrupoles		
MQG1F03	first telescope	-693.6744938
MQG1F04	|	0
MQG1F05	|	500.9871344
MQB2F01	|	-655.1370219
MQB2F02	|	1310.274044
MQB2F03	V	-655.1370219
MQB2F04	second telescope	-2119.560953
MQB2F05	|	2408.591992
MQB2F06	|	-1252.467836
MQG2F07	|	905.6305891
MQG2F08	|	-481.7183984
MQG2F09	V	192.6873594
MQH3F01	first end loop trims	0
MQH3F02	|	0
MQH3F03	|	0
MQH3F04	V	0
MQG4F01	backleg	134.4015836
MQG4F02	|	631.4181097
MQG4F03	|	-659.3379917
MQG4F04	|	683.2443829
MQG4F05	|	-659.8578256
MQG4F06	|	659.8578256
MQG4F07	|	-659.8578256
MQG4F08	|	659.8578256
MQG4F09	|	-659.8578256
MQG4F10	|	683.2443829

MQG4F11	|	-659.3379917
MQG4F12	|	631.4181097
MQG4F13	V	134.4015836
MQH5F01	second end loop trims	0
MQH5F02	|	0
MQH5F03	|	0
MQH5F04	V	0
MQB5F05	re-injection telescope	96.34367969
MQB5F06	|	0
MQB5F07	|	770.7494375
MQB5F08	V	-578.0620781

Table 2: Re-matched Optics with Rudimentary Energy Compression

magnet or string	description	bl (g-cm) or b'l (g)
dipoles		
MDU1F02	extraction string	11018.49869
MDW2F01	optical cavity string	47952.11301
MDX3F01	first reverse bend	65148.80351
MDX2G01	trim on first reverse bend	set to 0 current
MDY3F03	C-bend	403563.4618
quadrupoles		
MQG1F03	first telescope	-693.6744938
MQG1F04	|	0
MQG1F05	|	500.9871344
MQB2F01	|	-655.1370219
MQB2F02	|	1310.274044
MQB2F03	V	-655.1370219
MQB2F04	second telescope	-2119.560953
MQB2F05	|	2370.05452
MQB2F06	|	-1252.467836
MQG2F07	|	905.6305891
MQG2F08	|	-500.9871344
MQG2F09	V	192.6873594
MQH3F01	first end loop trims	0
MQH3F02	|	-32.75685109
MQH3F03	|	-32.75685109
MQH3F04	V	0
MQG4F01	backleg	134.4015836
MQG4F02	|	631.4181097

MQG4F03	|	-659.3379917
MQG4F04	|	683.2443829
MQG4F05	|	-659.8578256
MQG4F06	|	659.8578256
MQG4F07	|	-659.8578256
MQG4F08	|	659.8578256
MQG4F09	|	-659.8578256
MQG4F10	|	683.2443829
MQG4F11	|	-659.3379917
MQG4F12	|	631.4181097
MQG4F13	V	134.4015836
MQH5F01	second end loop trims	0
MQH5F02	|	-32.75685109
MQH5F03	|	-32.75685109
MQH5F04	V	0
MQB5F05	re-injection telescope	96.34367969
MQB5F06	|	57.80620781
MQB5F07	|	770.7494375
MQB5F08	V	-578.0620781